Industrial Chemistry & Materials

ROYAL SOCIETY OF CHEMISTRY

PAPER

View Article Online
View Journal | View Issue

Cite this: *Ind. Chem. Mater.*, 2025, **3**, 464

Green recovery of all-solid-state sodium-ion batteries/lithium-ion batteries by ionic liquids, deep eutectic solvents and low-melting mixture solvents

Yu Chen, * Guojian Zhao, Jiayi Dong, Jing Wang, Dexin Dong, Zheng Li, Mengxi Zhao, Zhuojia Shi and Zihang Niu

All-solid-state sodium-ion batteries (ASIBs) have good application prospects due to the high energy density, high safety and long lifetime. The excessive use of ASIBs in the near future will inevitably lead to the generation of spent batteries, contributing to environmental pollution and resource waste. In this work, we utilize three types of green solvents—ionic liquids (ILs), deep eutectic solvents (DESs), and low-melting mixture solvents (LoMMSs)—to recover both the cathode and solid electrolyte from ASIBs, as well as the cathode and electrolyte from lithium-ion batteries (LIBs). Results show that the leaching efficiency of Na from the cathode and solid electrolyte of ASIBs by LoMMSs could respectively reach as high as 92.8% and 96.7% at a mild temperature of 80 °C, which is higher than that in ILs and DESs. The highest metal leaching efficiency from ASIBs is similar to that from LIBs. Both LoMMSs and leachate are non-flammable when exposed to a high-temperature torch. In addition, 70 anti-solvents are screened to recover metal from the leachate at room temperature, with acetone yielding the highest precipitation efficiency of 92.0%.

Keywords: Green solvents; Rechargeable batteries; Solid waste; Green chemistry; Physical properties; Anti-solvents.

Received 21st November 2024,
Accepted 21st May 2025

DOI: 10.1039/d4im00149d

rsc.li/icm

1 Introduction

Sodium-ion batteries (SIBs),[1,2] lithium-ion batteries (LIBs),[3–6] zinc-ion batteries (ZIBs),[7,8] aluminium-ion batteries (AIBs),[9] potassium-ion batteries (PIBs),[10–12] and magnesium-ion batteries (MIBs)[13,14] are among the most widely studied and discussed energy storage technologies in recent decades. Although LIBs have seen the greatest commercialization success, their safety and cost remain a concern. In contrast, sodium-ion batteries (SIBs) are starting to enter the market, driven by their advantages of safety, lower cost, and abundant raw materials.[1,2,15] In particular, all-solid-state sodium-ion batteries (ASIBs) containing solid electrolytes hold significant potential for battery applications due to their higher energy density and improved safety.[16] However, toxic and expensive cathode and solid electrolyte materials in ASIBs, coupled with their excessive use in the near future, could potentially lead to environmental pollution and depletion of metal resources.[17] Therefore, it is crucial to develop a new approach for the green and efficient recovery of waste ASIBs.

Green solvents include water, supercritical fluids, ionic liquids (ILs), deep eutectic solvents (DESs) and low-melting mixture solvents (LoMMSs).[18] Water and supercritical fluids are traditional green solvents, whereas ILs, DESs, and LoMMSs can be considered novel green solvents. Although water is cheap, sustainable, and renewable, it has limited solubility for the cathode and solid electrolyte in batteries. Supercritical fluids are difficult to generate at mild temperatures and are often expensive and energy-intensive when used for ASIB recycling. ILs are ionic salts that remain in a liquid state near room temperature,[19] distinguishing them from both molecular liquids and ionic solids. The properties of ILs can be highly tailored through variations in cation types, anion types, interactions, and two- or three-dimensional steric configurations.[20,21] ILs are extensively used in electrochemistry, separation processes, catalysis, and LIB recycling.[22–29] However, to date, there have been no reports on the use of ILs for the recovery of ASIBs to the best of our knowledge.

DESs are eutectic mixtures that exhibit a greater melting-point depression than the ideal liquidus.[30] Since their discovery in 2003 by Abbott *et al.*,[31] the interactions in DESs have expanded beyond the primary hydrogen bonding (between the hydrogen bond donor (HBD) and the hydrogen bond acceptor

Department of Chemistry and Material Science, Langfang Normal University, Langfang 065000, Hebei, China. E-mail: yuchen@iccas.ac.cn

(HBA)) to include halogen bonding, host–guest interactions, non-covalent forces, and other complex molecular interactions.[32–38] Although DESs are considered designable green solvents in the 21st century,[39] they also have several limitations,[30,40,41] including their misleading name, lack of phase diagrams, challenges with recyclability, and debated environmental impact. Currently, many researchers are focused on biomass utilization, gas capture, industrial separation, and particularly on the recovery of LIBs using DESs.[42–47] Nevertheless, the use of DESs in ASIB recycling is limited.[48] For example, the DESs polyethylene glycol 200 : ascorbic acid can achieve a maximum Na leaching efficiency of 88.3% from the cathode and solid electrolyte of ASIBs.[48]

The concept of LoMMSs is proposed by Yu's group in 2023, which broadens the field of green solvents and green chemistry.[49] The term "LoMMSs" refers to mixtures that have a lower melting point than their individual components and remain in a liquid state at operating temperature, functioning as solvents. In contrast to DESs, LoMMSs do not require the "deep" or "eutectic" characteristics, which are difficult to achieve and rarely demonstrated in the existing literature. In fact, DESs are a specific type of LoMMSs characterized by deep and eutectic properties. Since their discovery in 2023, LoMMSs have found a wide range of applications in environmental and energy fields.[50–54] To date, LoMMSs have been highlighted as promising green solvents for recycling ASIBs in a single report. Specifically, Chen *et al.* showed that nearly 100% Na leaching efficiency could be achieved using natural LoMMSs, composed of choline chloride (ChCl) as the HBA and glucose, catechol, or *p*-hydroxybenzyl alcohol as the HBD.[50]

Here, we use three kinds of novel green solvents (ILs, DESs and LoMMSs) to recycle cathode materials and electrolytes of ASIBs. Sodium iron phosphate ($Na_4Fe_3(PO_4)_2P_2O_7$, NFP, 42 500 RMB per kg), Prussian white ($Na_2Mn[Fe(CN)_6]$, NMF, 3000 RMB per kg) and sodium vanadium phosphate ($Na_3V_2(PO_4)_3$, NVP, 40 000 RMB per kg) are selected as the representative cathodes of ASIBs; ceramic powder ($Na_3Zr_2Si_2PO_{12}$, NZSP) is chosen as the typical solid electrolyte of ASIBs owing to its relatively high price of 36 000 RMB per kg. The chemical compositions of DESs, ILs, and LoMMSs are presented in Fig. 1a, while the leaching process is illustrated in Fig. 1b. ChCl serves as the HBA while urea act as the HBD in DESs, as evidenced by a reliable solid–liquid phase diagram for ChCl : urea[55] systems. ChCl : ethylene glycol (EG) is not considered a DES as demonstrated by previous reports[56–58] but it could be classified as a LoMMS. Glucose (GLU) and lactic acid (LA) are respectively the HBA and HBD in LoMMSs, as indicated by the absence of a V-shaped solid–liquid phase diagram with a horizontal solidus for the GLU : LA system. The cations of ILs include 1-butyl-3-methylimidazolium ([BMIM]), 1-hexyl-3-methylimidazolium ([HMIM]) and 1-octyl-3-methylimidazolium ([OMIM]), while the anions are tetrafluoroborate ($[BF_4]$) and hexafluorophosphate ($[PF_6]$).

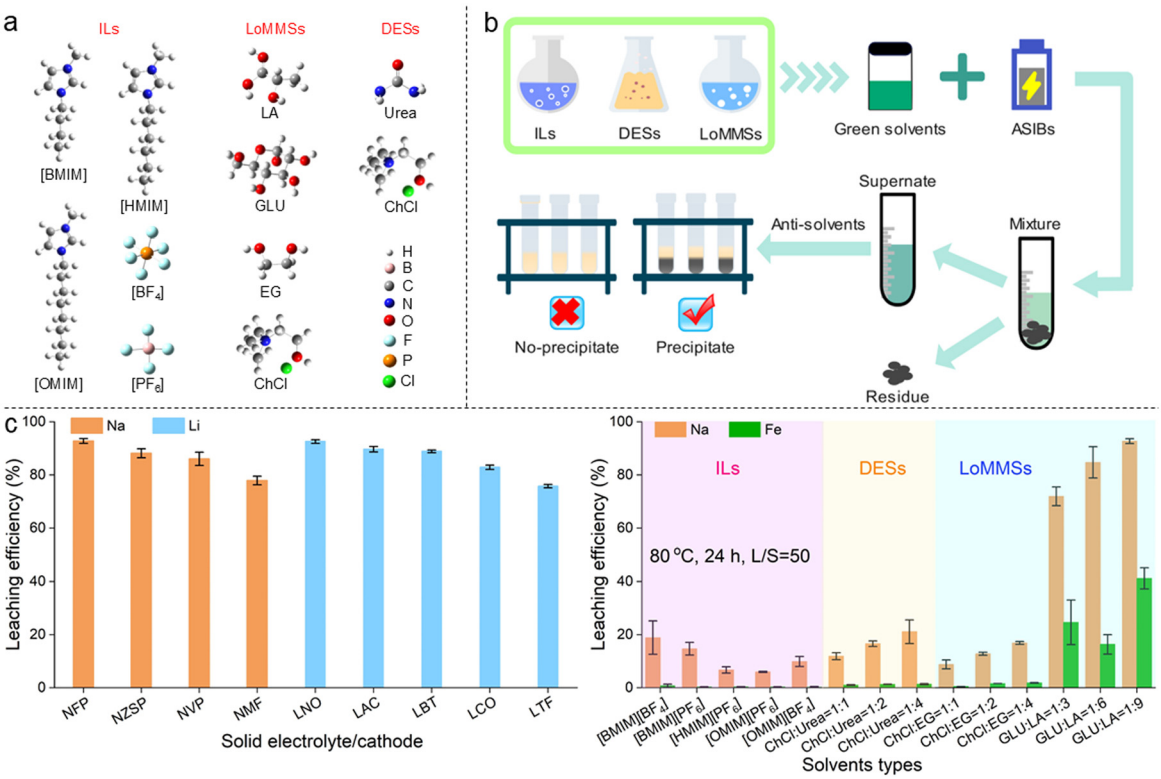

Fig. 1 Chemical structures of the three types of novel green solvents ILs, DESs and LoMMSs (a), process for ASIB recovery (b), metal leaching efficiency from batteries affected by waste type (80 °C, 24 h, 0.1 g waste from ASIBs or LIBs, 5 g LoMMS GLU : LA (1 : 9)) and by green solvent types (80 °C, 24 h, 0.1 g NFP cathode from ASIBs, 5 g solvent) (c).

2 Results and discussion

2.1 Effect of waste type

Cathode materials such as NFP, NMF and NVP, along with the solid electrolyte NZSP, are chosen as representatives for ASIBs. In LIBs, the cathode materials are lithium cobalt oxide (LCO) and lithium nitrate (LNO), while the typical electrolyte components include lithium acetate (LAC), lithium bis(trifluoromethylsulfonyl)azanide (LBT), and lithium tetrafluoroborate (LTF). Fig. 1c and Table 1 show that the Na leaching efficiency for ASIBs is in the order NFP (92.8%) > NZSP (88.2%) > NVP (86.1%) > NMF (77.9%) by LoMMS GLU : LA (1 : 9) at 80 °C for 24 h, while the Li leaching efficiency order is LNO (92.6%) > LAC (89.7%) > LBT (88.9%) > LCO (82.9%) > LTF (75.8%) for LIBs. It could be concluded that the highest Na leaching efficiency (92.8% NFP) from ASIBs is comparable to that of Li leaching efficiency (92.6%, LNO) from LIBs. Additionally, the Na/Fe separation ratio from NFP using LoMMS GLU : LA (1 : 9) could reach 2.3 when the maximum Na leaching efficiency is achieved. Given the promising potential for widespread application of ASIBs in the near future, we select the ASIB cathode NFP with the highest Na leaching efficiency for the following investigation.

2.2 Effect of solvent type

ILs, DESs and LoMMSs are selected as the representative novel green solvents for the recovery of ASIB cathode NFP at 80 °C for 24 h. According to Fig. 1c and Table 2, the Na leaching efficiency by ILs follows the order [BMIM][BF_4] (18.9%) > [BMIM][PF_6] (14.7%) > [OMIM][BF_4] (9.9%) > [HMIM][PF_6] (6.7%) > [OMIM][PF_6] (6.0%). This suggests that ILs with a higher alkyl chain length would decrease the Na leaching efficiency as demonstrated by the order [BMIM][BF_4] (18.9%) > [OMIM][BF_4] (9.9%) and [BMIM][PF_6] (14.7%) > [HMIM][PF_6] (6.7%) > [OMIM][PF_6] (6.0%). In addition, the Na leaching efficiency by BF_4-based ILs are greater than those by PF_6-based ILs (*e.g.*, [BMIM][BF_4] (18.9%) > [BMIM][PF_6] (14.7%)). The possible reasons for higher Na leaching efficiency by BF_4-based ILs than PF_6-based counterparts might be the lower solid–liquid transition temperature and lower viscosity of [BMIM][BF_4].[59] Furthermore, the HBA basicity β of [BMIM][BF_4] is higher than that of [BMIM][PF_6].[60] This indicates that [BMIM][BF_4] has a greater coordinating ability with NFP, resulting in a higher Na leaching efficiency by [BMIM][BF_4] than by [BMIM][PF_6].

For all the three types of novel green solvents (ILs, DESs and LoMMSs), Na leaching efficiency from NFP is much higher than Fe leaching efficiency. LoMMS GLU : LA (1 : 9) has the highest leaching efficiency for both Na (92.8%) and Fe (41.2%) when compared to DESs and ILs investigated. Therefore, LoMMS GLU : LA (1 : 9) is selected as the solvent to optimize.

For DES ChCl : urea with different mole ratios (1 : 1, 1 : 2 and 1 : 4), increasing the HBD (*i.e.*, urea) concentration enhances the Na leaching efficiency from NFP (Fig. 2a and Table 2). Similarly, a higher content of HBD (*e.g.*, EG in ChCl : EG or LA in GLU : LA) in LoMMSs results in higher Na leaching efficiency. Similarly, for ASIB cathode NVP containing precious V, a higher content of HBD (*e.g.*, EG in ChCl : EG or LA in GLU : LA) in LoMMSs leads to both Na and V leaching efficiency (Fig. 2e). However, leaching efficiency of precious metals V and Zr from ASIB solid electrolyte NZSP is negligible when the HBD content in LoMMSs varies (Fig. 2e). Unexpectedly, Na leaching efficiency from solid electrolyte NZSP increases with a lower content of HBD LA in GLU : LA and reaches the highest value of 96.7% by GLU : LA (1 : 3) (Fig. 2e).

2.3 Effect of temperature

Temperature plays an important role in the leaching of Na and Fe from NFP by LoMMSs. The leaching concentrations of Na in NFP by LoMMS GLU : LA (1 : 9) at 25 °C, 40 °C, 60 °C, 80 °C and 100 °C are 2249.3 ppm, 2383.7 ppm, 2314.0 ppm,

Table 1 Effects of the cathode/solid electrolyte on metal leaching efficiency by LoMMS GLU : LA (1 : 9)

Battery type	Cathode or electrolyte	1 (%)	2 (%)	3 (%)	4 (%)	Separation ratio
		η_{Na}	η_{Fe}			$\eta_{Na/Fe}$
ASIBs	NFP	92.8 ± 0.9	41.2 ± 4.0			2.3
		η_{Na} (%)	η_{Zr} (%)			$\eta_{Na/Zr}$
ASIBs	NZSP	88.2 ± 1.7	2.3 ± 0.2			38.3
		η_{Na}	η_{V}			$\eta_{Na/V}$
ASIBs	NVP	86.1 ± 2.5	96.0 ± 2.7			0.9
		η_{Na}	η_{Fe}	η_{Mn}		$\eta_{Na/Fe}$, $\eta_{Na/Mn}$
ASIBs	NMF	77.9 ± 1.6	0.7 ± 0.03	0.5 ± 0.06		111.3, 155.8
		η_{Li}				
LIBs	LNO	92.6 ± 0.7				
		η_{Li}				
LIBs	LAC	89.7 ± 1.0				
		η_{Li}				
LIBs	LBT	88.9 ± 0.5				
		η_{Li}	η_{Co}			$\eta_{Li/Co}$
LIBs	LCO	82.9 ± 0.8	2.4 ± 0.0			34.5
		η_{Li}				
LIBs	LTF	75.8 ± 0.6				

Table 2 Effects of solvent types, temperature, time and solvent mass on metal leaching from NFP[a]

Variable	Condition	c_{Na} (ppm)	η_{Na} (%)	c_{Fe} (ppm)	η_{Fe} (%)	$\eta_{Na/Fe}$
	ILs [BMIM][BF_4]	671.3 ± 233.1	18.9 ± 6.3	49.5 ± 39.8	0.8 ± 0.6	23.6
	ILs [BMIM][PF_6]	593.5 ± 96.9	14.7 ± 2.4	23.4 ± 1.9	0.3 ± 0.03	49.0
	ILs [HMIM][PF_6]	255.7 ± 45.2	6.7 ± 1.2	24.8 ± 2.8	0.4 ± 0.04	16.8
	ILs [OMIM][PF_6]	218.2 ± 8.0	6.0 ± 0.2	21.6 ± 3.1	0.3 ± 0.05	20.0
	ILs [OMIM][BF_4]	323.0 ± 61.2	9.9 ± 1.9	15.7 ± 10.9	0.3 ± 0.2	33.0
	DES ChCl : Urea (1 : 1)	399.2 ± 34.8	11.9 ± 1.3	55.6 ± 1.2	1.0 ± 0.2	11.9
	DES ChCl : Urea (1 : 2)	584.0 ± 36.1	16.6 ± 1.0	84.2 ± 5.5	1.3 ± 0.1	12.8
	DES ChCl : Urea (1 : 4)	791.3 ± 166.6	21.1 ± 4.4	91.7 ± 15.2	1.3 ± 0.2	16.2
	LoMMSs ChCl : EG (1 : 1)	282.6 ± 43.6	8.8 ± 1.7	27.8 ± 1.2	0.5 ± 0.02	17.6
	LoMMSs ChCl : EG (1 : 2)	431.8 ± 6.4	12.8 ± 0.6	96.6 ± 0.2	1.6 ± 0.004	8.0
	LoMMSs ChCl : EG (1 : 4)	556.0 ± 17.7	16.9 ± 0.5	111.4 ± 6.5	1.9 ± 0.1	8.9
	LoMMS GLU : LA (1 : 3)	2786.2 ± 136.0	71.9 ± 3.5	1739.3 ± 593.1	24.7 ± 8.4	2.9
	LoMMS GLU : LA (1 : 6)	3160.5 ± 219.9	84.7 ± 5.9	1111.3 ± 247.8	16.4 ± 3.6	5.2
	LoMMS GLU : LA (1 : 9)	3400.5 ± 33.2	92.8 ± 0.9	2750.8 ± 266.2	41.2 ± 4.0	2.3
Time (h)	0.17	1649.7 ± 160.5	45.0 ± 4.4	1455.7 ± 145.9	21.8 ± 2.2	2.1
	1	2965.8 ± 22.9	80.9 ± 0.6	1425.3 ± 126.7	21.3 ± 1.9	3.8
	6	3369.0 ± 61.5	90.7 ± 0.04	2253.0 ± 34.0	33.7 ± 0.5	2.7
	12	3355.5 ± 110.3	91.5 ± 3.0	2191.5 ± 14.8	32.8 ± 0.2	2.8
	24	3400.5 ± 33.2	92.8 ± 0.9	2750.8 ± 266.2	41.2 ± 3.9	2.3
	36	3666.3 ± 73.2	100.0 ± 1.9	2763.3 ± 353.2	41.4 ± 5.3	2.4
T (°C)	25	2249.3 ± 210.3	61.4 ± 5.7	1018.5 ± 75.6	15.2 ± 1.1	4.0
	40	2383.7 ± 63.1	65.0 ± 1.7	2131.8 ± 124.8	31.9 ± 1.9	2.0
	60	2314.0 ± 104.7	63.1 ± 2.8	1971.7 ± 132.3	29.5 ± 2.0	2.1
	80	3400.5 ± 33.2	92.8 ± 0.9	2750.8 ± 266.2	41.2 ± 4.0	2.3
	100	3408.8 ± 30.8	93.0 ± 0.8	1145.7 ± 255.8	17.2 ± 3.8	5.4
LoMMSs mass (g)	5	3400.5 ± 33.2	92.8 ± 0.9	2750.8 ± 266.2	41.2 ± 3.9	2.3
	15	1140.8 ± 1.06	93.3 ± 0.08	1180.0 ± 42.7	53.0 ± 1.9	1.8
	20	865.8 ± 34.5	94.4 ± 3.7	1070.7 ± 65.3	64.1 ± 3.9	1.5
Magnification	1×	3400.5 ± 33.2	92.8 ± 0.9	2750.8 ± 266.2	41.2 ± 3.9	2.3
	100×	2900.3 ± 322.8	79.1 ± 8.8	798.5 ± 8.3	12.0 ± 0.1	6.6

[a] The detailed conditions are listed below: effects of solvent types (5 g solvents, 0.1 g NFP, 80 °C, 24 h), temperature (5 g LoMMS GLU : LA (1 : 9), 0.1 g NFP, 24 h), time (5 g LoMMS GLU : LA (1 : 9), 0.1 g NFP, 80 °C), mass of LoMMS GLU : LA (1 : 9) (0.1 g NFP, 80 °C, 24 h), magnification (80 °C, 24 h, LoMMS GLU : LA (1 : 9), NFP).

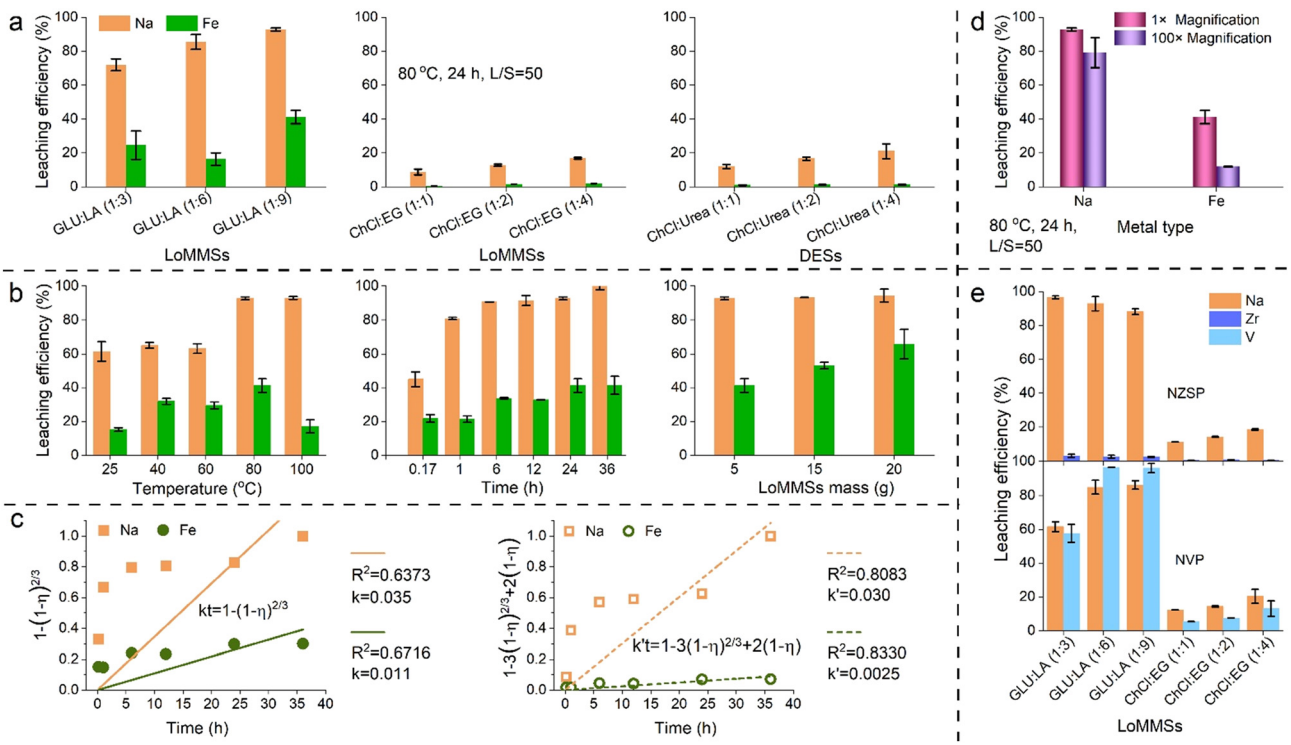

Fig. 2 Effect of mole ratio (a), and time, temperature and LoMMS mass (b) on Na and Fe leaching from NFP by LoMMSs. Kinetic regression of metal leaching (c). Scale-up experiment (d). Metal leaching from NZSP and NVP by LoMMSs GLU : LA and ChCl : EG (e).

3400.5 ppm and 3408.8 ppm, respectively (Table 2 and Fig. 2b). Correspondingly, the leaching efficiencies of Na from NFP by LoMMSs are 61.4%, 65.0%, 63.1%, 92.8% and 93.0%, respectively. We can conclude that Na leaching efficiency generally increases with the temperature. At 100 °C, LoMMSs have the highest Na leaching efficiency from the NFP cathode. Fe leaching efficiencies from NFP by LoMMSs are 15.2%, 31.9%, 29.5%, 41.2% and 17.2% at 25 °C, 40 °C, 60 °C, 80 °C and 100 °C, respectively. Under the condition of 80 °C, LoMMSs have the highest Fe leaching efficiency. However, the Na/Fe selectivity is the highest when the temperature is 100 °C. Data at 120 °C are not discussed because the supernatant could not be extracted for analysis due to the carbonization.

2.4 Effect of time

Table 2 and Fig. 2b show that the Na leaching concentrations at 0.17 h, 1 h, 6 h, 12 h, 24 h and 36 h are 1649.7 ppm, 2965.8 ppm, 3369.0 ppm, 3355.5 ppm, 3400.5 ppm and 3666.3 ppm, respectively; similarly, the Na leaching efficiencies are 45.0%, 80.9%, 90.7%, 91.5%, 92.8% and 100%, respectively. It could be concluded that both Na leaching concentration and leaching efficiency increases with time. The Fe leaching efficiencies at 0.17 h, 1 h, 6 h, 12 h, 24 h and 36 h are 21.8%, 21.3%, 33.7%, 32.8%, 41.2% and 41.4%, respectively, which also display an increasing tendency. In all circumstances, the Na leaching efficiency is much higher than the Fe leaching efficiency. The Na/Fe selectivity reaches the highest value at a moderate time point of 1 h when both Na (80.9%) and Fe (21.3%) leaching efficiencies are relatively low. Kinetic regression of metal leaching[48,50] suggests that the surface chemical reaction-controlled process (R^2_{Na} = 0.6373, R^2_{Fe} = 0.6716) is less favorable than the diffusion-controlled process (R^2_{Na} = 0.8083, R^2_{Fe} = 0.8330) because the R^2 values of the former is lower (Fig. 2c).

2.5 Effect of mass

When the mass of LoMMSs increases, both Na and Fe leaching efficiencies gradually increase as shown in Table 2 and Fig. 2b. For example, the Na leaching efficiencies are 92.8%, 93.3%, and 94.4% when the LoMMS masses are 5 g (L/S = 50), 15 g (L/S = 150) and 20 g (L/S = 200), respectively. Similarly, the Fe leaching efficiencies are 41.2%, 53.0% and 64.1%, respectively. The Na leaching efficiency is much higher than the Fe leaching efficiency in all the LoMMS masses investigated. Moreover, the selectivity is in the order $\eta_{Na/Fe}$ (5 g) > $\eta_{Na/Fe}$ (15 g) > $\eta_{Na/Fe}$ (20 g). Although a higher LoMMS mass leads to higher Na leaching efficiency, the difference is less than 6%. Therefore, we select 5 g for the optimization after considering both Na/Fe selectivity and Na leaching efficiency.

2.6 Large-scale application

The scalability of leaching processes is a crucial factor in determining whether LoMMSs can be applied on an industrial scale. Table 2 shows that as the magnification increases from 1 to 100 times, the leaching efficiency of Na only slightly decreases (from 92.8% to 79.1%), while the leaching efficiency of Fe drops from 41.2% to 12.0%. Although the metal leaching efficiency decreases in different degrees, the selectivity for Na/Fe increases from 2.3% to 6.6%. This indicates that the scalable leaching is beneficial for the selective and efficient recovery of Na metal from ASIBs using LoMMSs. Therefore, the leaching process of LoMMSs for recovering materials from ASIBs could be applied to the industrial recycling of spent ASIBs.

2.7 Comparison

In this work, GLU : LA (1 : 9) achieves a Na leaching efficiency of 90.1% from NFP cathode materials under the conditions of 80 °C for 6 h. Chen *et al.*[48] used PEG200 : ascorbic acid (14 : 1) at 80 °C for 24 h, achieving a Na leaching efficiency of 63.5% from NMF cathode materials. Compared with PEG200 : ascorbic acid, GLU : LA (1 : 9) in this work efficiently recovers Na from cathode materials within a shorter time. Biomass-based LoMMSs achieve a Na leaching efficiency of up to 99% from NZSP solid electrolytes under conditions of 80 °C for 24 h.[50] However, the relatively long processing time of biomass-based LoMMSs for Na recovery from solid electrolytes reduces its practicality for large-scale applications. Chen *et al.*[61] used a PEG200 : phytic acid-based LoMMS (14 : 1) at 80 °C for 6 h, and the Na leaching efficiency (76.1%) is much lower than that of GLU : LA-based LoMMSs (90.1%) in this work. Biomass-based vegetable/fruit-derived solvents demonstrate relatively low Na leaching efficiencies in the recovery of Na from cathode materials.[62] In summary, GLU : LA-based LoMMSs achieve mild, rapid and efficient recovery of Na from cathode materials compared with the above green solvents.

2.8 Properties and mechanism

Regulating the physical properties of LoMMSs can improve their leaching efficiency for recovering NFP cathode materials from ASIBs. The density and electrical conductivity of the leachate are both higher than those of LoMMSs (Fig. 3a). This indicates that the valuable metals in the NFP cathode material are dissolved by the LoMMSs, leading to an increase in density and electrical conductivity. The surface tension of the leachate is slightly higher than that of the LoMMSs, which could be due to the attraction of NFP by LoMMSs into the bulk phase rather than the surface phase after dissolution. This further supports that the kinetic behavior of LoMMSs dissolving the cathode material follows the inert layer diffusion model. The viscosity of the leachate is significantly higher than that of the LoMMSs, indicating that GLU : LA effectively recovers metals from NFP.[54] The pH follows the order: leachate > LoMMSs > LA. The increase in the pH of the leachate may result from acid–base interactions between the acidic LoMMSs and the basic NFP cathode material.[54] It is observed that the IR of leachate shows only slight peak shifts when compared to

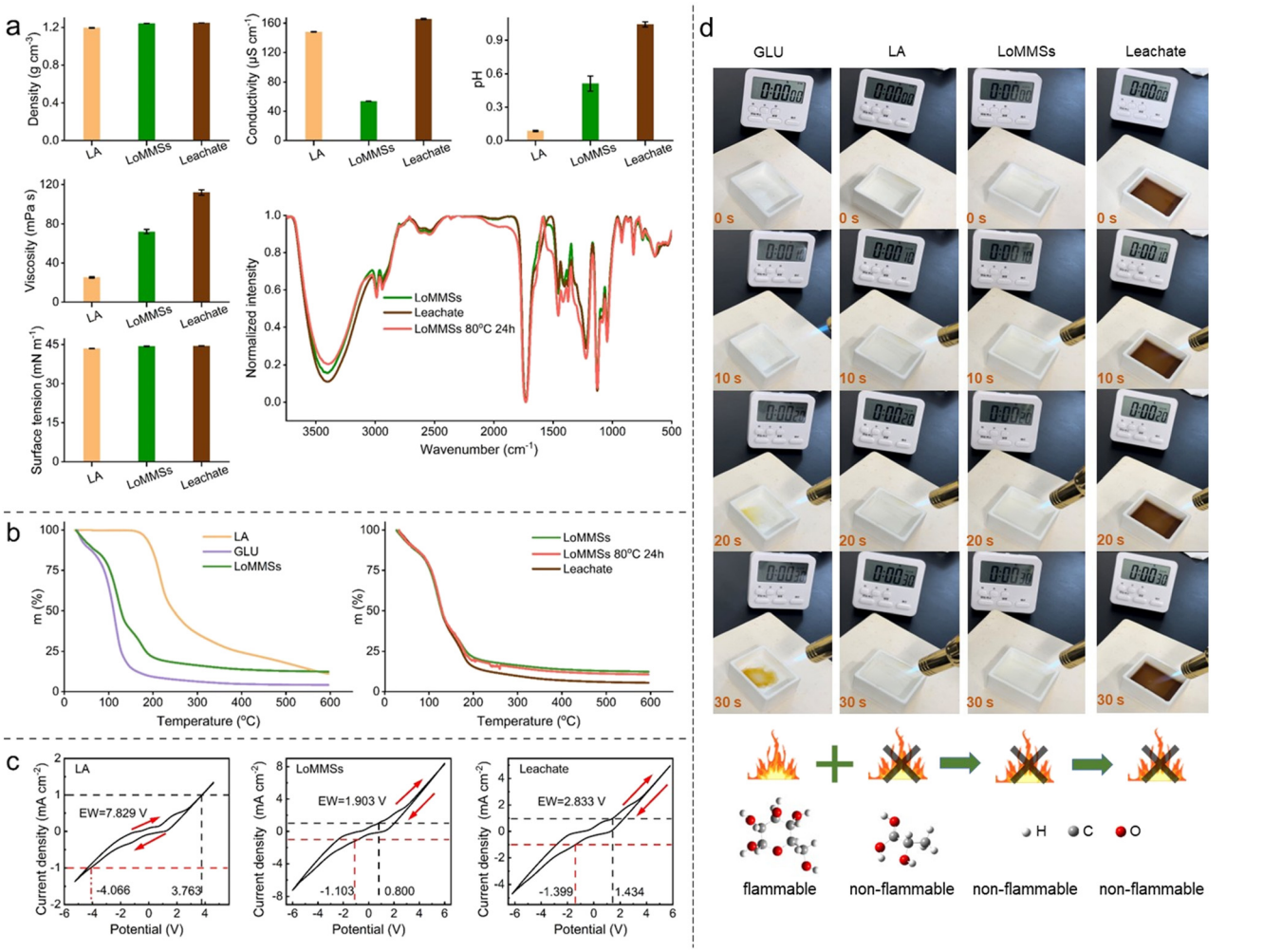

Fig. 3 Density, electrical conductivity, pH, viscosity, surface tension, and IR spectra (a), TGA curves (b), and cyclic voltammograms (c) of LA, LoMMSs and leachate. Details for cyclic voltammetry: 100 mV s^{-1} scan rate, Pt counter electrode, GC working electrode, SCE reference electrode, 1 mA cm^{-2} cutting-off current density. Combustion of GLU, LA, LoMMSs and leachate (d).

the IR of LoMMSs, with no increase in the number of peaks or changes in peak shapes. Therefore, it is inferred that there is no redox interaction between LoMMSs and the NFP cathode material, while other interactions (*i.e.*, physical interactions, acid–base interactions and coordination interactions) may be present.[48]

The stability of LoMMSs is one of the key factors for dissolving the cathode material NFP. The order of T_{onset} values in Fig. 3b is as follows: 190.46 °C (LA) > 105.12 °C (LoMMSs) > 103.68 °C (leachate) > 103.24 °C (heating LoMMSs at 80 °C for 24 h) > 92.96 °C (GLU). This indicates that prolonged heating has little effect on the T_{onset} of LoMMSs, suggesting that they possess good thermal stability. The high thermal stability of LoMMSs could be corroborated by the negligible change in IR (Fig. 3a) and $^{1}H/^{13}C$ NMR (Fig. 4) spectra when comparing LoMMSs before and after heating at 80 °C for 24 h. Fig. 3d shows that both LoMMSs and leachate are non-flammable, indicating that the recovery process of cathode material NFP by LoMMSs is safe and reliable.

Fig. 3c shows that the electrochemical window of the leachate is larger than that of LoMMSs. This suggests that the electrochemical stability of the leachate is higher than that of LoMMSs. Under the condition of a cut-off current density of 1 mA cm^{-2}, the reduction potentials of LoMMSs (higher) and the leachate (lower) are −1.103 V *vs.* SCE and −1.399 V *vs.* SCE, respectively. This indicates that the reduction ability of the leachate becomes higher after the metal leaching by LoMMSs. Therefore, we could deduce that no redox reaction is involved for the dissolution of the cathode material NFP by LoMMSs because the reduction ability would decrease if the redox reaction dominates the dissolution process. The trend in reduction potential is consistent with the findings about biomass-based vegetable/fruit-derived solvents by Chen *et al.*[62] IR spectra (Fig. 3a) and $^{1}H/^{13}C$ NMR spectra (Fig. 4) of the leachate show no new peaks when compared to LoMMSs, further supporting the exclusion of the redox interaction between LoMMSs and the cathode material.

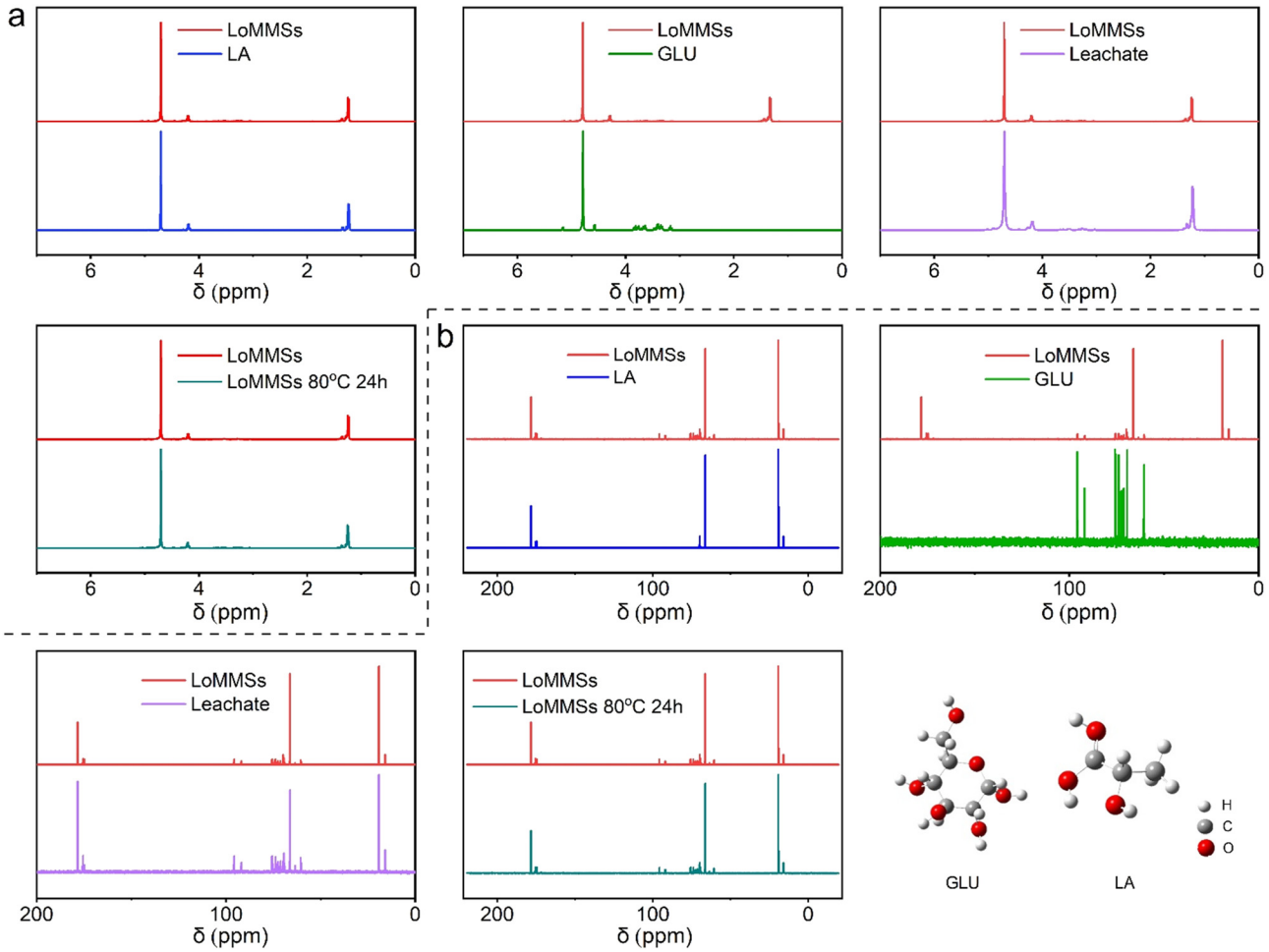

Fig. 4 ^{1}H NMR (a) and ^{13}C NMR spectra (b) of components, LoMMSs, heated LoMMSs at 80 °C for 24 h, and leachate in D_2O.

2.9 Precipitation by anti-solvents

70 anti-solvents are used at room temperature to separate Na and Fe from the leachate in the form of precipitation. Table 3 shows that only 12 anti-solvents successfully separate Na and Fe from the leachate. Fig. 5 shows that the order of precipitation efficiency for Na among the 12 anti-solvents is: acetone (92.0%) > tetrahydrofuran (90.9%) > ethylene glycol diethyl ether (90.1%) > 1,4-dioxane (90.0%) > 2-methyl-3-butyn-2-ol (88.5%) > acetonitrile (84.9%) > *n*-propanoic acid (83.9%) > benzyl alcohol (83.3%) = isopropanol (83.3%) > 5-norbornene-2-methanol (81.3%) > propylene carbonate (81.2%) > malononitrile (80.3%). The Fe precipitation efficiency by the 12 anti-solvents ranges approximately from 20% to 32%. This indicates that the anti-solvents could selectively and efficiently separate Na from the leachate in the form of precipitation, while retaining Fe in the leachate.

3 Conclusions

In summary, the leaching efficiency of Na from the cathode and solid electrolyte of ASIBs by LoMMSs is higher than that by ILs and DESs. The highest metal leaching efficiency from ASIBs is similar to that from the cathode and electrolyte of LIBs. Na leaching efficiency from the NFP cathode using GLU : LA (1 : 9) after 100 time scale up only shows a slight decrease (from 92.8% to 79.1%). The leachate exhibits higher density, conductivity, viscosity, surface tension and pH compared to LoMMSs. In addition, LoMMSs demonstrate good thermal stability and nonflammability. Acetone could be used as an anti-solvent to achieve the highest precipitation efficiency of 92.0% at room temperature after screening 70 kinds of anti-solvents.

4 Materials and methods

4.1 Materials and instruments

GLU (AR) and LA (80–85%) were provided by Beijing Innochem Co., Ltd; Na standard solution (1000 ppm), Fe standard solution (1000 ppm), Zr standard solution (1000 ppm), Mn standard solution (1000 ppm) and V standard solution (1000 ppm) were supplied by National Nonferrous Metals. [BMIM][BF_4] (97%), [BMIM][PF_6] (95%), [HMIM][PF_6] (97%) and [OMIM][PF_6] (95%) were acquired from Shanghai Macklin Biochemical Technology Co., Ltd; ChCl was

Table 3 Recovery of leachate using 70 anti-solvents

No.	Anti-solvents	Prec.[a]	No.	Anti-solvents	Prec.[a]
1	1,4-Dioxane	■	37	PEG200	○
2	1,5-Diazabicyclo [4.3.0] 5-nonene	○	38	PEG600	○
3	1,8-Diazabicyclo [5.4.0]undec-7-ene	○	39	Phytic acid	○
4	*n*-Propanol	○	40	Benzene	○
5	Collodion	○	41	Lactic acid	○
6	2-Methyl-3-butyn-2-ol	■	42	Diisopropylamine	○
7	5-Norbornene-2-methanol	■	43	Trichloromethane	○
8	5-Norbornene-2-carboxylic acid	○	44	Triethylamine	○
9	*N*,*N*-Dimethylformamide	○	45	Triethanolamine	○
10	*N*-Methyl pyrrolidone	○	46	Petroleum ether	○
11	*N*-Methyl acetamide	○	47	Hydrazine hydroxide	○
12	Ammonium hydroxide	○	48	Bu_4NOH (25% in H_2O)	○
13	Aniline	○	49	Hydrobromic acid	○
14	Phenol	○	50	Cyclohexane	○
15	Benzyl alcohol	■	51	Tetrahydrofuran	■
16	Pyridine	○	52	Propylene carbonate	■
17	Acetic acid	○	53	Bu_4NOH (40% in methanol)	○
18	Malononitrile	■	54	Formic acid	○
19	Edible oil	○	55	Ethanol	○
20	Glycerol	○	56	Ether	○
21	Acetone	■	57	Ethylene glycol	○
22	Dichloromethane	○	58	Ethylene glycol diethyl ether	■
23	Dimethyl silicone oil	○	59	Acetonitrile	■
24	Ethyl acetate	○	60	*p*-Tolualdehyde	○
25	Dimethyl sulfoxide	○	61	Butyl acetate	○
26	Levulinic acid	○	62	Acetic anhydride	○
27	Isopropanol	■	63	Hydrogen peroxide	○
28	$[BMIM][PF_6]$	○	64	Acetylacetone	○
29	*n*-Propanoic acid	■	65	$[OMIM][PF_6]$	○
30	Butyl titanate	○	66	$[BMIM][BF_4]$	○
31	Cyclopentane	○	67	PEG300	○
32	Epichlorohydrin	○	68	Decanoic acid	○
33	Lubricating oil	○	69	pentane	○
34	Toluene	○	70	Water	○
35	Methanol	○	71	Blank experiment	○
36	Methyl tertiary-butyl ether	○			

[a] Prec. is the abbreviation for precipitation. The symbol ■ means precipitation. The symbol ○ means that there is no precipitation observed.

purchased from Beijing Jingming Biotechnology Co., Ltd. EG (≥99%) and urea (≥99%) were purchased from Shanghai Aladdin Biochemical Technology Co., Ltd. NFP (AR), NVP (AR) and NZSP (AR) were supplied by Shenzhen Kejing Zhida Technology Co., Ltd. The anti-solvents used for precipitation and the instruments for property analysis were the same as those in our previous reports.[48,50,54,63]

4.2 Leaching process and scalability

Typically, 0.1 g of the cathode (or solid electrolyte) and 5 g of ILs (DESs or LoMMSs) were heated and stirred at 80 °C for 24 h. The resulting mixtures were then transferred to a centrifuge tube and centrifuged at 12000 rpm for 20 minutes. The supernatant was carefully collected into a clean glass bottle to obtain the leachate. Finally, the leachate was analyzed using ICP-OES (Fig. 1). For scale-up applications, the LoMMSs and NFP processes were scaled up by a factor of 100, utilizing 10 g of cathode NFP and 500 g of solvents, compared to the initial conditions of 0.1 g of cathode and 5 g of solvents at 80 °C for 24 h.

4.3 Leaching efficiency and properties

Eqn (1) is used to calculate the concentration of metals.

$$\eta_x = \frac{cm/\rho}{M_x} \times 100\% \quad (1)$$

η_x: leaching efficiency of metal element x. c: leaching concentration of metal elements in the supernatant by ICP-OES. m: mass of DESs, ILs or LoMMSs. ρ: density of DESs, ILs or LoMMSs. M_x: mass of metal element x in the material.

4.4 Properties and spectra

The specific usage information of the properties and spectra (*i.e.*, manufacturer, model, *etc.*) is consistent with the research we reported previously.[48,64,65]

Data availability

The data that support the findings of this study are available from the corresponding author upon reasonable request.

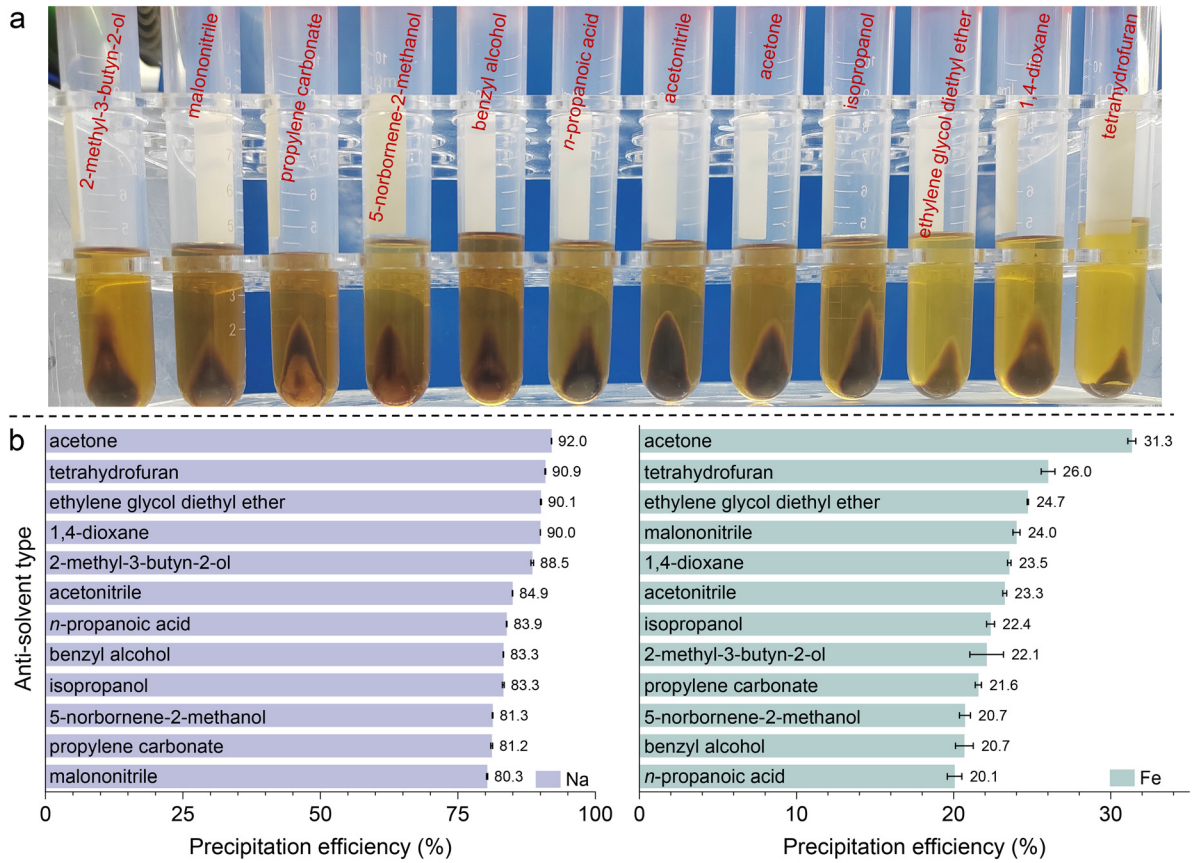

Fig. 5 Precipitation observed (a) and precipitation efficiency (b) for the recovery of metals from leachate using 70 anti-solvents.

Conflicts of interest

There are no conflicts to declare.

Acknowledgements

This work was supported by the Natural Science Foundation of Hebei Province/S&T Program of Hebei (B2024408022), the National Natural Science Foundation of China (22103030), and the Natural Science Foundation of Hebei Province (B2024408003).

References

1 M. Xu, M. Liu, Z. Yang, C. Wu and J. Qian, Research progress on presodiation strategies for high energy sodium-ion batteries, *Acta Phys.-Chim. Sin.*, 2022, **39**, 2210043.

2 M. Aranda, P. Lavela and J. L. Tirado, A novel potassium-containing layered oxide for the cathode of sodium-ion batteries, *Battery Energy*, 2024, **3**, 20230057.

3 T. Qin, H. Yang, Q. Li, X. Yu and H. Li, Design of functional binders for high-specific-energy lithium-ion batteries: from molecular structure to electrode properties, *Ind. Chem. Mater.*, 2024, **2**, 191–225.

4 G. F. I. Toki, M. K. Hossain, W. U. Rehman, R. Z. A. Manj, L. Wang and J. Yang, Recent progress and challenges in silicon-based anode materials for lithium-ion batteries, *Ind. Chem. Mater.*, 2024, **2**, 226–269.

5 L. Wang, H. Dang, T. He, R. Liu, R. Wang and F. Ran, Dual-functional and polydopamine-coated vanadium disulfide for "fast-charging" lithium-ion batteries, *Battery Energy*, 2024, **3**, 20240001.

6 G. Luo, M. He, L. Zhang, J. Deng, L. Chen, Y. Chao, H. Liu, W. Zhu and Z. Liu, Enhanced lithium extraction from brine using surface-modified $LiMn_2O_4$ electrode with nanoparticle islands, *Ind. Chem. Mater.*, 2025, **3**, 353–362.

7 R. Jin, Y. Fang, B. Gao, Y. Wan, Y. Zhou, G. Rui, W. Sun, P. Qiu and W. Luo, Copper ions-intercalated manganese dioxide self-supporting mesoporous carbon electrode for aqueous zinc-ion batteries, *Ind. Chem. Mater.*, 2025, **3**, 87–96.

8 J. Ren, H.-Y. Wu, W. Yan, P. Huang and C. Lai, Stable zinc anode by regulating the solvated shell and electrode–electrolyte interface with a sodium tartrate additive, *Ind. Chem. Mater.*, 2024, **2**, 328–339.

9 X. Wang, Z. Xi and Q. Zhao, Progress on aqueous rechargeable aluminium metal batteries, *Ind. Chem. Mater.*, 2024, **3**, 7–30.

10 X. Niu, N. Li, Y. Chen, J. Zhang, Y. Yang, L. Tan, L. Wang, Z. Zhang, S. S. Fedotov, D. Aksyonov, J. Wu, L. Guo and Y. Zhu, $K_2[(VOHPO_4)_2(C_2O_4)]\cdot 2H_2O$ as a high-potential cathode material for potassium-ion batteries, *Battery Energy*, 2024, **3**, 20240006.

11 B.-J. Xin and X.-L. Wu, Research progresses on metal-organic frameworks for sodium/potassium-ion batteries, *Battery Energy*, 2024, **3**, 20230074.
12 Y. Xu, Y. Du, H. Chen, J. Chen, T. Ding, D. Sun, D. H. Kim, Z. Lin and X. Zhou, Recent advances in rational design for high-performance potassium-ion batteries, *Chem. Soc. Rev.*, 2024, **53**, 7202–7298.
13 Y. Man, P. Jaumaux, Y. Xu, Y. Fei, X. Mo, G. Wang and X. Zhou, Research development on electrolytes for magnesium-ion batteries, *Sci. Bull.*, 2023, **68**, 1819–1842.
14 Y. Man, Y. Fei, L. Duan, R. Tian, A. Li, Z. Yuan and X. Zhou, Self-assembled vanadium oxide nanoflowers as a high-efficiency cathode material for magnesium-ion batteries, *Chem. Eng. J.*, 2023, **472**, 145118.
15 S.-W. Kim, D.-H. Seo, X. Ma, G. Ceder and K. Kang, Electrode materials for rechargeable sodium-ion batteries: Potential alternatives to current lithium-ion batteries, *Adv. Energy Mater.*, 2012, **2**, 710–721.
16 X. Lin, S. Zhang, M. Yang, B. Xiao, Y. Zhao, J. Luo, J. Fu, C. Wang, X. Li, W. Li, F. Yang, H. Duan, J. Liang, B. Fu, H. Abdolvand, J. Guo, G. King and X. Sun, A family of dual-anion-based sodium superionic conductors for all-solid-state sodium-ion batteries, *Nat. Mater.*, 2025, **24**, 83–91.
17 M. J. Baumann, J. Peters, M. Häringer, M. Schmidt, L. Schneider, W. Bauer, J. R. Binder and M. Weil, Prospective hazard and toxicity screening of sodium-ion battery cathode materials, *Green Chem.*, 2024, **26**, 6532–6552.
18 J. Hu, J. Zhang, Y. Zhao and Y. Yang, Green solvent systems for material syntheses and chemical reactions, *Chem. Commun.*, 2024, **60**, 2887–2897.
19 L. A. Blanchard, D. Hancu, E. J. Beckman and J. F. Brennecke, Green processing using ionic liquids and CO_2, *Nature*, 1999, **399**, 28–29.
20 D. Dai, B. Cao, X.-L. Hao and Z.-W. Yu, Transition mechanism from the metastable two-dimensional gel to the stable three-dimensional crystal of imidazolium-based ionic liquids, *J. Phys. Chem. B*, 2023, **127**, 7323–7333.
21 D. Dai, B. Cao, X.-L. Hao, Z.-H. Li and Z.-W. Yu, Free-standing two-dimensional crystals formed from self-assembled ionic liquids, *J. Phys. Chem. Lett.*, 2023, **14**, 2744–2749.
22 X. Ma, J. Yu, Y. Hu, J. Texter and F. Yan, Ionic liquid/poly(ionic liquid)-based electrolytes for lithium batteries, *Ind. Chem. Mater.*, 2023, **1**, 39–59.
23 Y. Li, F. Li, A. Laaksonen, C. Wang, P. Cobden, P. Boden, Y. Liu, X. Zhang and X. Ji, Electrochemical CO_2 reduction with ionic liquids: review and evaluation, *Ind. Chem. Mater.*, 2023, **1**, 410–430.
24 W. Tu, S. Zeng, Y. Bai, X. Zhang, H. Dong and X. Zhang, Theoretical insights into NH_3 absorption mechanisms with imidazolium-based protic ionic liquids, *Ind. Chem. Mater.*, 2023, **1**, 262–270.
25 M. Wang, Y. Wang, Y. Han, H. Dong, F. Huo and H. He, Bio-inspired polyionic membrane for long-lasting and repeatable electricity harvesting from moisture, *Nano Energy*, 2024, **123**, 109376.
26 Y. Han, Y. Wang, M. Wang, H. Dong, Y. Nie, S. Zhang and H. He, Nanofluid-guided janus membrane for high-efficiency electricity generation from water evaporation, *Adv. Mater.*, 2024, **36**, 2312209.
27 X. Gao, J. Zhao, Y. Gao, Y. Deng, Y. Shi, J. He and Y. Li, Benoxazolone-based Ionic liquid catalyzed C–S bond construction for synthesis of benzothiazoles from 2-aminothiophenols and CO_2 under ambient conditions, *New J. Chem.*, 2023, **47**, 17449–17455.
28 M. Sheng, X. Zhang, H. Cheng, Z. Song and Z. Qi, Multi-criteria computational screening of [BMIM][DCA]@ MOF composites for CO_2 capture, *Green Chem. Eng.*, 2024, **6**, 200–208.
29 L. Sun, L. Chai, L. Jing, Y. Chen, K. Zhuo and J. Wang, 2,6-Diaminoanthraquinone modified Mxene (Ti_3C_2Tx)/graphene as the negative electrode materials for ionic liquid-based asymmetric supercapacitors, *Green Energy Environ.*, 2024, **10**, 845–853.
30 M. A. R. Martins, S. P. Pinho and J. A. P. Coutinho, Insights into the Nature of Eutectic and Deep Eutectic Mixtures, *J. Solution Chem.*, 2019, **48**, 962–982.
31 A. P. Abbott, G. Capper, D. L. Davies, R. K. Rasheed and V. Tambyrajah, Novel solvent properties of choline chloride/urea mixtures, *Chem. Commun.*, 2003, 70–71, DOI: **10.1039/b210714g**.
32 P. Kalhor, K. Ghandi, H. Ashraf and Z. Yu, The structural properties of a ZnCl2–ethylene glycol binary system and the peculiarities at the eutectic composition, *Phys. Chem. Chem. Phys.*, 2021, **23**, 13136–13147.
33 P. Kalhor, Y.-Z. Zheng, H. Ashraf, B. Cao and Z.-W. Yu, Influence of hydration on the structure and interactions of ethaline deep-eutectic solvent: A spectroscopic and computational study, *ChemPhysChem*, 2020, **21**, 995–1005.
34 P. Kalhor, X. Jing, H. Ashraf, B. Cao and Z.-W. Yu, Structural properties and hydrogen-bonding interactions in binary mixtures containing a deep-eutectic solvent and acetonitrile, *J. Phys. Chem. B*, 2020, **124**, 1229–1239.
35 D. Yu, H. Mou, H. Fu, X. Lan, Y. Wang and T. Mu, "Inverted" deep eutectic solvents based on host-guest interactions, *Chem. – Asian J.*, 2019, **14**, 4183–4188.
36 D. Yu, H. Mou, X. Zhao, Y. Wang and T. Mu, Eutectic molecular liquids based on hydrogen bonding and π-π interaction for exfoliating two-dimensional materials and recycling polymers, *Chem. – Asian J.*, 2019, **14**, 3350–3356.
37 D. Yu and T. Mu, Strategy to form eutectic molecular liquids based on noncovalent interactions, *J. Phys. Chem. B*, 2019, **123**, 4958–4966.
38 R. Shi, D. Yu, F. Zhou, J. Yu and T. Mu, An emerging deep eutectic solvent based on halogen-bonds, *Chem. Commun.*, 2022, **58**, 4607–4610.
39 A. Paiva, R. Craveiro, I. Aroso, M. Martins, R. L. Reis and A. R. C. Duarte, Natural deep eutectic solvents - solvents for the 21st century, *ACS Sustainable Chem. Eng.*, 2014, **2**, 1063–1071.

40 Y. Chen and T. Mu, Revisiting greenness of ionic liquids and deep eutectic solvents, *Green Chem. Eng.*, 2021, **2**, 174–186.
41 D. O. Abranches and J. A. P. Coutinho, Everything you aanted to know about deepeutectic solvents but were afraid to be told, *Annu. Rev. Chem. Biomol. Eng.*, 2023, **14**, 141–163.
42 M. Hu, B. Han, L. Xie, B. Lu, D. Bai, N. Shi, Y. Liao, Y. Wang, L. Liu, S. Wu, R. Lan, X. Lei, C. Shi, D. Huang, Y. Li, L. Lin and J. Zhang, Ultrasonic assisted natural deep eutectic solvents as a green and efficient approach for extraction of hydroxytyrosol from olive leaves, *Ind. Chem. Mater.*, 2024, **2**, 309–320.
43 L. Li, X. Li, S. Zhang, H. Yan, X. Qiao, H. He, T. Zhu and B. Tang, Increasing the greenness of an organic acid through deep eutectic solvation and further polymerisation, *Green Energy Environ.*, 2022, **7**, 840–853.
44 Y. Bao, Y. Wang, C. Yan and Z. Xue, Deep eutectic solvents for fractionation and valorization of lignocellulose, *Green Chem. Eng.*, 2025, **6**, 21–35.
45 H. X. Han, L. Chen, J. C. Zhao, H. T. Yu, Y. Wang, H. L. Yan, Y. X. Wang, Z. M. Xue and T. C. Mu, Biomass-based acidic Deep eutectic solvents for efficient dissolution of lignin: Towards performance and mechanism elucidation, *Acta Phys.-Chim. Sin.*, 2023, **39**, 2212043.
46 L. Y. Zhang, H. T. Yu, S. Liu, Y. Wang, T. C. Mu and Z. M. Xue, Kamlet-taft parameters of deep eutectic solvents and their relationship with dissolution of main lignocellulosic components, *Ind. Eng. Chem. Res.*, 2023, **62**, 11723–11734.
47 Q. Liu, X. Zhao, D. Yu, H. Yu, Y. Zhang, Z. Xue and T. Mu, Novel deep eutectic solvents with different functional groups towards highly efficient dissolution of lignin, *Green Chem.*, 2019, **21**, 5291–5297.
48 Y. Chen, Y. Shen, Z. Shi, Z. Zhang, Q. Zhang, Y. Wang, M. Feng and C. Wang, Recovery of all-solid-state sodium-ion batteries cathode and solid electrolyte using deep eutectic solvents as green solvents, *Sep. Purif. Technol.*, 2025, **359**, 130473.
49 Y. Chen and Z. Yu, Low-melting mixture solvents: Extension of deep eutectic solvents and ionic liquids for broadening green solvents and green chemistry, *Green Chem. Eng.*, 2024, **5**, 409–417.
50 Y. Chen, Y. Shen, Z. Liu, M. Yang, Y. Zhang, Z. Niu, Y. Wang, M. Feng and Z. Shi, Natural low-melting mixture solvents for green recovery of spent all-solid-state sodium-ion batteries with superior efficiency over lithium-ion batteries, *ChemSusChem*, 2025, **18**, e202402457.
51 N. Alomari, A. Maletta, S. Aparicio, A. Gutiérrez and M. Atilhan, Elucidating the dynamics behavior of PFASs at the water and hydrophobic low-melting mixture solvents interphase, *J. Mol. Liq.*, 2024, **407**, 125170.
52 G. A. Bracchini, S. D. Muzio, F. Trequattrini, O. Palumbo, A. Paolone and F. Ramondo, Fatty acid and alcohol based low melting mixtures: The role of intermolecular interactions by DFT and infrared spectroscopy, *J. Mol. Liq.*, 2025, **417**, 126590.
53 P. Kalhor, Z. Sun and Z. Yu, Spectroscopic and computational study of zncl$_2$–methanol low-melting-temperature mixtures, *J. Phys. Chem. B*, 2024, **128**, 2490–2503.
54 Y. Chen, H. Liang, Q. Zhang, G. Zhao, Z. Liu, Y. Guo, Z. Yang, T. Wang and J. Chen, Simultaneously achieving high Li leaching efficiency and Li/Co selectivity from lithium-ion batteries cathode by using natural low-melting mixture solvents (LoMMSs) as green solvents, *Sep. Purif. Technol.*, 2025, **354**, 128967.
55 M. Gilmore, M. Swadzba-Kwasny and J. D. Holbrey, Thermal properties of choline chloride/urea system studied under moisture-free atmosphere, *J. Chem. Eng. Data*, 2019, **64**, 5248–5255.
56 H. J. Hayler and S. Perkin, The eutectic point in choline chloride and ethylene glycol mixtures, *Chem. Commun.*, 2022, **58**, 12728–12731.
57 R. Buchner and V. Agieienko, Ethaline and related systems: may be not "deep" eutectics but clearly interesting ionic liquids, *Pure Appl. Chem.*, 2023, **95**, 833–840.
58 V. Agieienko and R. Buchner, Is ethaline a deep eutectic solvent?, *Phys. Chem. Chem. Phys.*, 2022, **24**, 5265–5268.
59 N. Shamim and G. B. McKenna, Glass dynamics and anomalous aging in a family of ionic liquids above the glass transition temperature, *J. Phys. Chem. B*, 2010, **114**, 15742–15752.
60 J. Del Valle, F. García Blanco and J. Catalán, Empirical parameters for solvent acidity, basicity, dipolarity, and polarizability of the ionic liquids [BMIM][BF_4] and [BMIM][PF_6], *J. Phys. Chem. B*, 2015, **119**, 4683–4692.
61 Y. Chen, M. Zhao, J. Chen, J. Dong, Z. Niu, T. Wang, C. Wang and Y. Zhang, Green recovery of toxic prussian white cathode from spent all-climate sodium-ion batteries using low-melting mixture solvents (LoMMSs), *Battery Energy*, 2025, 20240091.
62 Y. Chen, Z. Yang, M. Zhao, X. Wang, D. Dong, Z. Niu, J. Dong and Z. Li, Green strategy for recycling spent all-solid-state sodium-ion batteries and kitchen waste using biomass-based vegetable-/fruit-derived solvents, *Sustainable Energy Fuels*, 2025, **9**, 2982–2992.
63 Y. Chen, Z. Shi, X. Zhang, C. Wang, Y. Wang, Z. Niu, Y. Zhang and M. Feng, Recycling solid electrolytes from all-solid-state lithium-ion batteries by using deep eutectic solvents as green extractants, *ChemSusChem*, 2025, **18**, e202402126.
64 Y. Chen, F. Zhang, H. Sun, Y. Chang, Z. Zhang, Z. Liu and M. Yang, Superlong supercooling solvents (SSSs): Alternative green solvents to ionic liquids and deep eutectic solvents for lithium-ion batteries recycling, *J. Mol. Liq.*, 2023, **391**, 123410.
65 Y. Chen, F. Zhang, Y. Chang, J. Wang, Q. Zhang, M. Yang, Z. Liu and Z. Zhang, Natural biomass soups (NBSs): New green solvents replacing ionic liquids and deep eutectic solvents for lithium-ion batteries recovery, *Energy Fuels*, 2023, **37**, 19076–19081.